Fuel 332 (2023) 125970

Contents lists available at ScienceDirect

Fuel

journal homepage: www.elsevier.com/locate/fuel

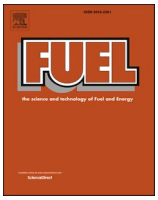

Thermochemical valorization of argan nutshells: Torrefaction and air–steam gasification

Zainab Afailal *, Noemí Gil-Lalaguna, Isabel Fonts, Alberto Gonzalo, Jesús Arauzo, José Luis Sánchez

Thermochemical Processes Group, Aragón Institute of Engineering Research (I3A), University of Zaragoza, C/Mariano Esquillor s/n, 50.018, Zaragoza, Spain

ARTICLE INFO

Keywords:
Argan nutshells
Waste valorization
Torrefaction
Air–steam gasification
Syngas quality

ABSTRACT

The upswing of argan's oil for the cosmetic industry has increased the farming of this plant and originated an unexplored residue of complex treatment, its nutshells. This work deals with the characterization of this feedstock, its pretreatment via torrefaction and its gasification either with or without the pretreatment stage. Torrefaction was carried out in a continuous auger reactor at two temperatures, 220 and 250 °C. Hemicellulose was almost totally removed from argan nutshells after torrefaction. Compared to the raw argan shells, the torrefied solids showed an increased content of fixed carbon, a noticeable reduction in the O/C ratio and a significant increase in the HHV, the higher the torrefaction temperature. Chemical thermodynamic equilibrium calculations were implemented to the gasification stage to calculate the equivalence ratio for auto-thermal operation and to assess the effect of temperature and steam-to-biomass ratio on gas yield and composition. Air-steam gasification was also experimentally tested for the raw and torrefied materials at the operational conditions drawn from the simulation results. The torrefied material gasification yielded four times more char than the raw material, while tar production from the torrefied material was only reduced in the presence of steam (anyway starting from a low value: 0.7 g/m^3_{STP} for raw argan shells vs 0.3 g/m^3_{STP} for the torrefied material). Nor gas production, neither the H_2/CO ratio nor the energy content in syngas were improved by gasifying the torrefied material, so torrefaction does not appear to be a profitable pretreatment stage for the gasification of argan nutshells from the point of view of syngas quality.

1. Introduction

Biomass is the most abundant and bio-renewable source of carbon and hydrogen on earth [1]. The transformation of biomass feedstocks is receiving growing attention as fundamental investigation lines in the field of sustainability and green energies, as well as on the finding of new sources and materials previously untapped. To benefit from biomass uses is a key point in the circular economy concept. It helps to reduce the generation of non-valorized residues and net emissions of greenhouse gases, and even the external energy dependence of particular regions, since the development of new strategies for the valorization of local biomasses could create new and clean industrial activities, thus contributing to the sustainable socio-economic development.

Argan's oil is increasingly highly valued directly or as an additive for cosmetic products, mainly produced by small rural cooperatives in Morocco. Its production is on the rise due to its boosting application in cosmetics and to its high price, up to 200 €/liter (2020). It is extracted from the fruit of the *Argania Spinosa (L.) Skeels*, an endemic tree of Morocco, covering about 870,000 ha in the country's south. The annual production of argan's oil is over 4,000 tons, leaving behind 20 tons of non-valorized waste (shells) per ton of oil produced [2]. Local people have tried to use this waste as a fuel for the traditional heating furnaces [3], but its hardness, rigidity, and difficulty in being ignited (delayed ignition and flame extinction [4]) prevent its easy and safe use in such a traditional way. The major macro-components of raw argan nutshells are cellulose, lignin, and hemicellulose, whereas minor ash and moisture contents are also present [3,5]. On a dry basis, the lignin content of this residue is up to 38 wt%. This high lignin content could be considered an intrinsic feature of most fruit shells, ranging between 38 and 45 wt% for almond and hazelnut shells [6,7]. Lower values of lignin content have usually been reported for hardwoods (18–25 wt%) and softwoods (25–35 wt%) [8].

* Corresponding author.
E-mail address: zainabafailal@unizar.es (Z. Afailal).

https://doi.org/10.1016/j.fuel.2022.125970
Received 29 January 2022; Received in revised form 26 August 2022; Accepted 8 September 2022
Available online 18 September 2022

Among the different valorization routes developed to efficiently convert lignin-rich biomass into biochemicals and biofuels, thermochemical processes are considered the most attractive pathway thanks to their faster kinetics. One of these thermochemical processes is gasification, which offers an interesting possibility of treatment in terms of conversion efficiency [9]. During gasification, a carbonaceous feedstock is converted into a gaseous fuel at high temperatures (typically in the range 800–1200 °C), using an oxidative medium, such as air, oxygen or steam [10]. The main product of gasification is the gas (usually referred to as syngas), which consists of a mixture of hydrogen (H_2), carbon monoxide (CO), carbon dioxide (CO_2), nitrogen (N_2) (if using air or enriched air as gasifying agent), methane (CH_4) and other light hydrocarbons. Clean syngas could be used as fuel for heat and/or power production due to its reasonable high energy density [11], but it seems even more attractive to evaluate its potential as a feedstock for Fisher-Tropsch-based processes to produce a great variety of liquid biofuels and biochemicals, such as methanol, ethanol and higher alcohols and dimethyl ether [12].

The synthesis of these biochemicals requires specific H_2/CO molar ratios, ranging from 2 for methanol to 1 for higher alcohols [13]. Steam is considered the simplest way to tune the gas composition [9]. Hence, the quality of syngas in terms of the H_2/CO ratio can be improved by using steam in the mixture of gasification agents, as has been highlighted by research works dealing with wood gasification [9,11]. However, this trend has been scarcely corroborated by works focused neither on lignin-rich biomass nor with pretreated biomass.

In addition to syngas, char (carbonaceous solid) and tar (mixture of heavy and condensable hydrocarbons) are also generated as by-products in this conversion process, thus constraining the gas production rate. Moreover, the existence of tar in the syngas negatively impacts its subsequent utilization by causing difficulties associated with condensation in downstream equipments, formation of aerosols and polymerization [14], and contribution to the deactivation of the catalysts used in the subsequent gas upgrading stages. In this regard, several studies in the literature outline that gasification accompanied by a previous torrefaction pretreatment of woody biomass could provide benefits such as reducing tar concentration in the gas [15–17], as the torrefied material has a decreased O/C ratio and volatile content, and a higher energy density and carbon content [9]. Cerone et al. stated that the use of torrefied Eucalyptus wood chips resulted in a fivefold lower tar concentration in the syngas (164 g/m^3 for the raw Eucalyptus wood chips vs 34 g/m^3 for the torrefied one) and a noticeable increment of the thermal power of the plant [15]. On the other hand, in the study of Kulkarni et al., a similar trend was observed in the gasification of torrefied pine, producing less than half of tar yield (8 g/ kg of raw dried pine vs 3.9 g/kg of torrefied pine) [17]. The effect of the torrefaction pretreatment on the production of tar in the gasification of such type of lignocellulosic materials seems to be clear. However, this effect has been scarcely studied for lignin-rich biomass, such as nutshells, and conclusions should not be directly extrapolated to these materials since lignin is known to be less affected by torrefaction than the carbohydrate fraction of lignocellulosic biomass [18].

An interesting study concerning argan nutshells combustion has recently been published [19], but, from the best of our knowledge, nothing more related to argan nutshells torrefaction or gasification has been published before. Therefore, the motivation of the current work is, on the one hand, to fill the gap in the literature concerning the characterization and the thermochemical upgrading of this type of biomass. On the other hand, to investigate new applications and end-uses for this waste, as well as to evaluate the technical feasibility at lab-scale before scaling up the process to be used on-site by the local producers for sustainable argan oil production. Recently published studies from our research group showed promising results on producing antioxidant additives [5] and catalyst supports [20] from argan nutshells. Like other similar agricultural residues, this material has a relatively high-energy content, making it a good candidate for thermochemical valorization. In the last decade, some studies have been dedicated to investigate the use of fruit shells in the gasification process using different reactors [11,21–24]. Yahaya et al. [24] studied air gasification of coconut and palm kernel shells at 700–900 °C, producing syngas with an H_2/CO ratio of 0.63–0.84 for coconut shells and 0.6–0.75 for palm kernel shells. On the other hand, Macrì et al. [25] stated that almond shells gasification theoretically exhibited more gas yield but lower cold gas efficiency compared with other feedstocks with high moisture content (microalgae, digestate and sludge).

In the present work, the gasification of torrefied argan nutshells, using air and air–steam as a gasifying agent, has been experimentally evaluated and compared with the raw biomass gasification performance in order to define the impact of such pretreatment on important gasification parameters. The main experimental results obtained in the torrefaction stage are also reported in this study to further explain the results observed in the gasification steps.

2. Materials and methods

2.1. Materials and characterization equipment

2.1.1. Raw material

The raw material employed in this torrefaction/gasification study is argan nutshells (AS), collected in the region of Essaouira (southwest of Morocco). AS was supplied by a Moroccan cooperative after removing the argan's nut. AS was milled and sieved in order to have a particle size of around 5 mm. The main characteristics of AS (as shown in section 3.1.2) are its considerable higher heating value (HHV = 19 MJ/kg), its low ash content (0.3 wt%), pretty similar cellulose and lignin contents (up to 35 wt%) and carbon content of 47.5 wt%.

2.1.2. Characterization equipment for solid materials

The raw material, as well as the solid products obtained in the torrefaction and gasification experiments, were characterized in terms of elemental composition, macro-components distribution and calorific value. The elemental analysis was determined using a LECO CHN628 Analyzer combined with the sulfur add-on module 628-S, while the proximate analysis, involving ash content, moisture content and volatile matter, was determined according to standard procedures (EN 14775:2010, EN 14774–3:2010 and EN 15148–2010, respectively). The organic extractives content was determined by the Soxhlet's extraction method using dichloromethane (DCM) as a solvent for 6 h. Hemicellulose, cellulose, and lignin contents were determined by the Van Soest analysis, which is based on subsequent digestion stages in different detergents (neutral detergent, acid detergent, and sulfuric acid 72 %) [26]. The solids' higher heating value (HHV) was measured using the IKA model C2000 basic calorific bomb.

The thermal behavior of the raw material and the torrefied solids was also investigated by thermogravimetric analysis (TGA-DTG, Proteus STA 449 F1 Jupiter-Netzsch). The thermogravimetric analysis (TGA) curves represent the instantaneous weight loss of a material during its thermal decomposition as a function of the applied temperature. Hence, this analysis can be a helpful tool to compare the chemical decomposition behavior of different materials, for example, the raw material and its torrefied solids obtained at different temperatures. During these experiments, around 50 mg of the solid sample was heated at a constant heating rate of 5 °C/min from ambient temperature to 700 °C; N_2 was used as a purge gas with a flow rate of 100 mL/min.

Surface functional groups on both the raw AS and the torrefied solids were investigated by Attenuated Total Reflection-Fourier Transform Infra-Red (ATR-FTIR) spectroscopy analysis, using an Agilent Cary 630 FTIR spectrometer, with a resolution of 4 cm^{-1} in the wavenumber range of 4000 – 400 cm^{-1} (medium IR region).

2.1.3. Characterization of liquid products

The composition of the liquid products obtained from either

torrefaction or gasification was also analyzed. Water content in the condensable liquids was measured using the Karl Fischer titration method (Mettler Toledo V-20 analyzer), and their densities were measured with a portable densimeter Mettler Toledo Densito 30px.

The composition of volatile compounds in the liquids was analyzed by gas chromatography (GC), using an Agilent 7890A GC chromatograph equipped with a flame ionization detector (FID) and combined with an Agilent 5975C mass selective detector (MSD) (operating parameters are listed in Table S1 in the Supplementary Information Section). The compounds identification and quantification were performed based on the peaks with more significant areas (> 92 % of the total area). Firstly, the identification of condensed organic compounds was performed using the MS signal by means of NIST MS Search Program 2.2. The quantification of those compounds was based on integrating the peaks of the FID signal.

For the torrefaction liquids, six standard solutions with 12 compounds each (acetol, furfural, 5-methylfurfural, 2-furanmethanol, guaiacol, creosol, phenol, 4-ethylguaiacol, eugenol, phenol 2,6-dimethoxy, vanillin, and acetic acid) were prepared in the concentration range of 240–4600 μg/mL, except for the acetic acid whose concentration range was higher (13323–91143 μg/mL). These standards were used for calibrating the FID signal. The FID response factors of other compounds that were also identified by GC/MS but not calibrated as standards were calculated from the response factor of the most similar standard compound used and applying to it a correction factor according to the methodology based on the Effective Carbon Numbers (ECN) [27] (more details about the calculation can be found in the Supplementary Information Section).

In the same way as torrefaction liquids, the composition of condensables from the gasification experiments was further analyzed. In this case, for the calibration of the FID signal, five calibration solutions were prepared in the concentration range of 10–500 μg/mL from different dilutions of a commercial standard containing 16 polycyclic aromatic hydrocarbons (PAH Mix 3 Supelco).

2.2. Torrefaction experimental setup

The torrefaction of AS was carried out in a laboratory-scale auger reactor (800 mm in length with an internal diameter of 55 mm) surrounded by an electrical furnace composed of three zones controlled separately. The schematic diagram of this system is presented in Fig. 1. The Auger reactor operated with continuous solid feeding and removal of volatiles using a flow of N_2 (1 L_{STP}/min) as inert carrier gas. The solid feeding rate and the solid residence time were both adjusted by varying the screw rotation frequency. These parameters were maintained constant at 5.4 g/min and 27 min, respectively (maximal rotation frequency of the screw). In each experiment, a total of 500 g of AS (particle size between 2 and 4 mm) was processed. The torrefied solid produced was collected in a recovering hopper situated at the end of the reactor (Fig. 1). A glass wool filter heated at the reactor's temperature was used to retain the small solid particles swept by the gas without condensing the vapors in this stage. Then, two condensers refrigerated with a water-ethylene glycol recirculating chiller (0.5 °C) were employed to collect the condensable vapors released during the reaction (water and organic compounds), followed by a cotton filter to finish cleaning the gas from traces of humidity and organics (1–2 % of the produced liquid was retained in the cotton filter). The particle- and organics-free gas volume was continuously measured using a volumetric gas meter (Gallus G4). The gas composition was analyzed online by a micro-gas chromatograph (Agilent 3000A), previously calibrated using a standard gas mixture of nine components (H_2, CH_4, CO, CO_2, C_2H_2, C_2H_4, C_2H_6, H_2S). The mass of each produced gas was calculated based on the composition data and the gas volume produced throughout the experiment.

Two different torrefaction temperatures (220 and 250 °C) were tested. As has already been reported in the literature, the torrefaction temperature has a more remarkable effect on the product distribution than other operational factors, such as the residence time [28]. For this reason, the temperature was the only operational factor studied in this work. For both treatment temperatures, consistent results were observed by duplication, with a reproducibility of the results < 10 % in the products yields.

Once the experiment had finished, the mass of the liquid product was determined by the weight difference of the condensers and the cotton filter before and after the experiment. To ensure a total recovery of the liquid collected in the condensers, whose composition will be analyzed, the condensers were washed with a weighted amount of solvent (methanol). On the other hand, the amount of torrefied solid was determined by the collecting hopper's weight difference (the reactor was empty at the end of the experiment).

The mass yields of gas, liquid and solid products ($Y_{m,i}$) were calculated with respect to biomass fed (Equation (1)). The total mass of biomass for these calculations was expressed on an as-received basis.

$$Y_{m,i} = \frac{Mass\ of\ solid,\ liquid\ or\ gas\ product\ (g)}{Total\ mass\ of\ biomass\ fed\ (g)} \bullet 100 \quad (1)$$

2.3. Gasification experimental setup

Gasification experiments of AS and argan shells torrefied at 220 °C (TAS220) were performed operating at atmospheric pressure in a lab-scale fluidized bed reactor (Fig. 2). Besides AS, TAS220 was chosen as gasification feedstock because of its higher production yield compared to the material torrefied at 250 °C (as shown in section 3.1.1). As the final particle size of TAS220 ranged between 2 and 4 mm, the raw AS fed to the gasification process was also crushed and sieved to a similar particle size for comparison purposes. Biomass was semi-continuously introduced into the reactor in the form of pulses of 3.5 g per minute through a double valve system placed at the top of the reactor. An initial

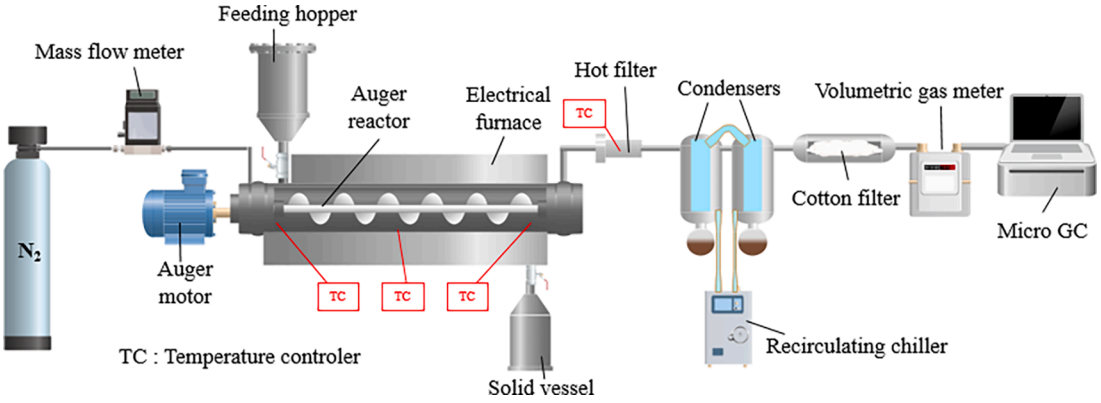

Fig. 1. Diagram of the torrefaction experimental setup.

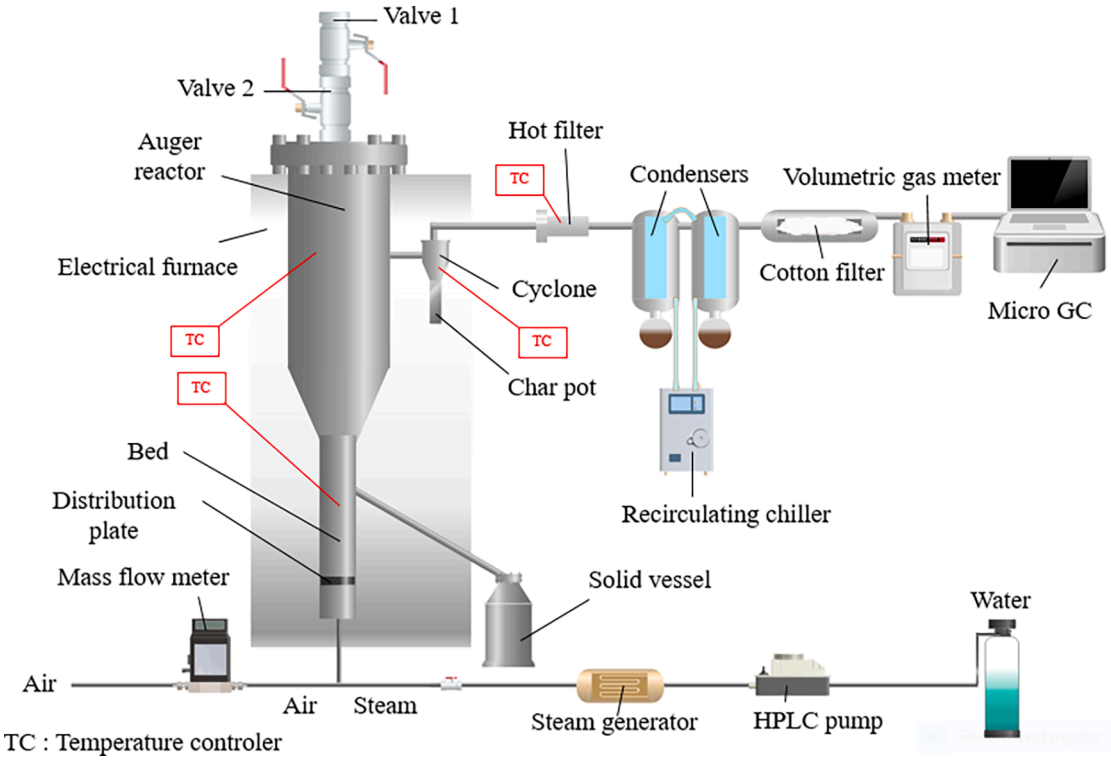

Fig. 2. Diagram of the gasification experimental setup.

bed (100 g) of calcined dolomite (at 900 °C) with a particle size of 350–500 μm was loaded. Using dolomite as bed material has been proved to report benefits in catalytic cracking of the generated tar [29]. The gasifying agent, composed of air or a mixture of air and steam, entered the reactor below the distributor plate and passed through the dolomite bed. Details about the reactor dimensions and the feeding systems for air and steam are explained elsewhere [14,30]. When solid in the reactor exceeded the available bed height, the solid (mixture of dolomite and char) left the bed overflowing to a solid container via a lateral pipe.

Vapors and gases passed through a cyclone and a glass wool filter (both heated to 450 °C), where the smallest solid particles (char and dolomite) were retained. Then, the condensing vapors and gas cleaning and analysis systems were similar to those in the torrefaction process (Section 2.2).

The lower heating value of the obtained syngas and the cold gas efficiency were calculated according to Equation (2) and Equation (3), respectively.

$$LHV_{gas} = \sum(x_i \cdot LHV_i) \quad (2)$$

where LHV_i (MJ/m^3_{STP}) is the lower heating value of each gaseous component and x_i its volumetric fraction (experimentally measured with the micro-gas chromatograph).

$$\text{Cold gas efficiency}\ (\%) = \frac{LHV_{gas} \bullet V_{gas}}{LHV_{feedstock} \bullet m_{feed}} \bullet 100 \quad (3)$$

where V_{gas} is the total volume of produced gas (m^3_{STP}), $LHV_{feedstock}$ is the lower heating value of the biomass fed (AS or TAS220), and m_{feed} is the total mass of biomass fed during the experiment (kg).

Each experiment was carried out for 60 min and, to estimate the experimental variability, each gasification run was repeated twice in the case of AS gasification.

2.4. Theoretical model for gasification

The gasification process has been theoretically modeled by studying the chemical equilibrium using HSC 9.0 software add-in in Excel. The calculations using the HSC 9.0 software were based on three conditions: i) minimization of the Gibbs free energy of the system, ii) compliance with the atomic balance in the whole process, and iii) establishment of an auto-thermal gasification reaction by accomplishing the energy balance without considering energy recovery from the products streams and taking into account 5 % of heat losses. By entering the characteristics of the raw material (mass flow, elemental analysis, ash and moisture contents and HHV), the gasification atmosphere composition (including S/C: steam to carbon mass ratio) and the expected gasification temperature, as well as other parameters related to the energy balance (calorific capacities and standard enthalpies of formation of reagents and products), the calculation procedure determined the required ER (equivalence ratio) in the gasification process for getting an auto-thermal reaction at a specific temperature. This simulation model also calculated the gas production and composition, fulfilling the aforementioned conditions. This model was run in a wide range of temperatures (750–1100 °C) and S/C ratios (up to 1.1 g H_2O/g biomass), and the results are detailed in Section 3.2.1.

The operational conditions for the experimental gasification runs were set based on these simulations results (Section 3.2.1) and are summarized in Table 1. Note that in the experiments in which the

Table 1
Operational conditions in the gasification experimental runs.

Run #	Feedstock	Gasifying agent	T (°C)	S/C	Added steam (L_{STP}/min)	ER (%)	Air flow (L_{STP}/min)
1, 2	AS	Air	850	0.184	0	31.1	6.2
3, 4	AS	Air-steam	850	0.5	0.7	32.2	6.4
5	TAS220	Air	850	0.024	0	33.4	7.9
6	TAS220	Air-steam	850	0.5	1.2	35.0	8.3

gasifying agent was only air (runs # 1, 2 and 5), the S/C ratio is not zero as it does not only refer to the added flow of steam but also includes the steam provided by the material moisture (g of moisture/ g of C). When feeding steam together with air as gasifying agent (runs # 3, 4 and 6), the S/C ratio of 0.5 includes both the material moisture and the flow of steam added.

3. Results and discussion

3.1. Torrefaction results

3.1.1. Products distribution

Mass balance closed fairly well, between 98 % and 99 %, in all the torrefaction experiments. Figure S1 in the Supplementary Information Section shows the distribution of the torrefaction products at 220 and 250 °C. Mass loss in the raw material increased with the torrefaction temperature as the devolatilization process promoted the formation of liquid and gas, thus decreasing the solid yield. The temperature is the main factor affecting the occurrence of the decomposition reactions [28], playing a pivotal role in kinetics, as can be seen in the strong effect on the product's yields even with an increase of only 30 °C. By increasing the temperature from 220 to 250 °C, the solid yield decreased from 65.8 to 49.7 wt%. Water was the second most abundant product after the torrefied solid and was obtained from either evaporation of moisture present in the material or dehydration reactions taking place with hydroxyl groups of carbohydrates (cellulose and hemicellulose) [28]. The water yield in AS torrefaction was 19.2 and 23.7 wt% at 220 °C and 250 °C, respectively. On the other hand, the yield of condensable organics with respect to biomass fed increased from 7.8 to 15.7 wt% when raising the temperature from 220 to 250 °C. The same upward trend was observed for non-condensable gas (from 5.4 to 10.4 wt %).

3.1.2. Characterization of torrefied solids

The product of interest in the torrefaction process is the torrefied solid, which should have better fuel properties than the raw material. The obtained solid (see its appearance in Figure S2 in the Supplementary Information Section) became darker with the increased temperature because of the caramelization of cellulose and hemicellulose components and the formation of quinones [31]. In addition, the high initial hardness of AS was noticeably reduced (the torrefied material was easily crushed). The results of ultimate and proximate analyses and the HHV of AS, TAS220, and TAS250 are summarized in Table 2. The HHV of AS increased from 18.6 MJ/kg to 22.7 MJ/kg in TAS220 and up to 27.0 MJ/kg in TAS250, meaning an increase of 22 % and 45 %, respectively. This energy density gain is ascribed to the release of volatiles [32] and increase in the fixed carbon content, and also consistent with the observed decrease in the O/C molar ratio in the torrefied solid due to the important release of CO_2 (section 3.1.3) and H_2O because of dehydration reactions. Table S2 in the Supplementary Information Section shows a comparison of AS torrefaction performance with other materials from the literature. For instance, in the study of Brachi et al. [33], the torrefaction of sugar beet pulp (smaller particle size between 1 and 2 mm and ash content up to 4 wt%) at 250 °C in a fixed bed reactor led to the same yield of solid product (49 wt%) but different production of gas (34.4 wt% for sugar beet pulp vs 10.4 wt% for AS) and liquid product (16.6 wt% for sugar beet pulp vs 39.4 wt% for AS) when operating at similar conditions but in different reactor type and particle size. For a shorter residence time (15 min vs 27 min in this work), higher torrefied solid yield (up to 83 wt% vs 49.7 wt% in this work) was reported in the study of Asadullah et al. [34] using palm kernel shell as raw material (bigger particle size between 7 and 15 mm and ash content of 3 wt%) in a fixed bed reactor. In contrast, in spite of using a woody material, whose behavior could be expected to be a priori far different from AS, Branchi et al. obtained a more similar value of solid yield (43 wt%) when torrefying pine (with closer particle size and ash content to AS) [35].

Table 2
Characterization results of AS, TAS220 and TAS250.

	AS	TAS220	TAS250
Proximate analysis (wt. %, ar. basis)			
Ash	0.20 ± 0.04	0.4 ± 0.1	0.73 ± 0.01
Moisture	8.74 ± 0.03	1.4 ± 0.4	2.0 ± 0.4
Volatile matter	74.6 ± 0.3	69 ± 2	52.6 ± 0.8
Fixed Carbon	16.5 ± 0.4	30 ± 2	45 ± 1
Ultimate analysis (wt. %, ar. basis)			
C	47.5 ± 0.2	59.8 ± 0.2	68.9 ± 0.1
H	6.55 ±	5.5 ± 0.1	4.75 ± 0.04
N	0.08	0.243 ±	0.33 ± 0.01
S	0.177 ±	0.005	0.040 ±
O[(a)]	0.003	0.040 ±	0.001
O/C ratio	0.044 ±	0.001	25.2 ± 0.1
H/C ratio	0.001	33.9 ± 0.3	0.28
	45.5 ± 0.2	0.43	0.43
	0.58	0.78	
	1.65		
HHV (MJ/kg)	18.61 ± 0.04	22.67 ± 0.04	26.97 ± 0.05
Macro-components composition (wt. %, ar. basis)			
Extractives	0.2 ± 0.1	0.4 ± 0.01	0.5 ± 0.1
Hemicellulose	21 ± 1	5 ± 0.2	0.60 ± 0.03
Cellulose	35 ± 2	31 ± 2	34 ± 2
Lignin	34 ± 2	61 ± 3	62 ± 3

(a) Calculated by difference (wt.%): O = 100—C—H—N—S—Ash.

Accordingly, the distribution of the products in the torrefaction process is impacted by many factors (reactor configuration, material nature, temperature, residence time, particle size and ash content) and extrapolating the results from one material to another does not result in good predictions if all the operational factors are not properly controlled.

Slight variations are also observed in the torrefied solid characteristics as, for example, HHV ranges between 22.7 and 26.2 MJ/kg and the carbon content between 60 and 70 wt%.

Table 2 also lists the results of the macro-components composition of the raw material and torrefied AS. The hemicellulose content dropped from 21 % in AS to 5 % in TAS220 and 0.6 % in TAS250. These results attest that hemicellulose was the major component decomposed during torrefaction, being almost totally degraded at 250 °C, which agrees with other results found in the literature [17]. The diminution of cellulose content was also significant in both cases: 41 % of cellulose in AS was degraded at 220 °C, and this rate increased to 51 % at 250 °C. These results highlight the high reactivity of this material even at this moderate temperature interval.

Regarding lignin, data in the literature show that its decomposition starts at around 200 °C [28]. Therefore, during torrefaction at 220–250 °C, lignin depolymerization should be expected to occur to some extent. In fact, as will be discussed below, the presence of some phenolic compounds in the torrefaction liquid points to the degradation of lignin. However, as shown in Table 2, the lignin content increased from 34 % in AS to 61 % in TAS220 and 62 % in TAS250. This increase was not only observed in terms of percentage but also in the net weight of lignin produced. This increase could be explained by the condensation and repolymerization processes of lignin itself during the torrefaction process [17] or due to the formation of new compounds from the decomposition of polysaccharides and subsequent condensation reactions, forming compounds that are insoluble in sulfuric acid (72 %) and therefore quantified as lignin by the Van Soest analysis procedure (considered as technical lignin).

The derivative thermogravimetry curves of AS, TAS220 and TAS250 are shown in Fig. 3. Different weight loss stages can be clearly distinguished in them. For the raw AS, the first low-intensity mass loss (up to 10 %) at the beginning of heating (T < 140 °C) corresponds to the removal of moisture (8.74 % according to the proximate analysis at

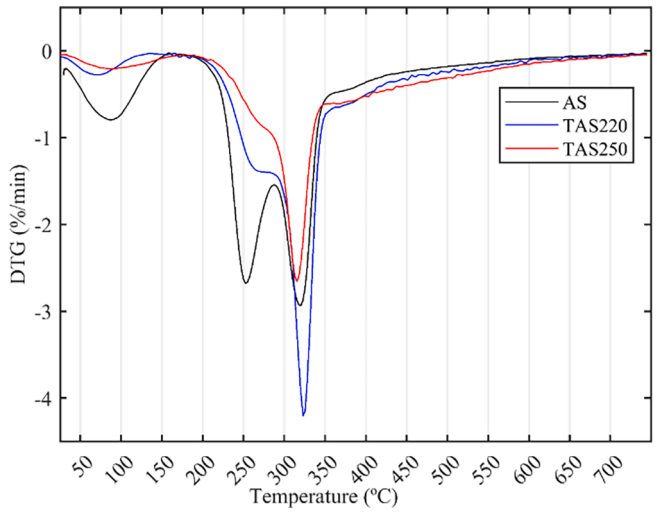

Fig. 3. DTG plots of AS before and after torrefaction at 220 and 250 °C.

105 °C); another stage of mass loss starts at around 200 °C, showing a strong intensity peak that continues up to around 350 °C. The slope change observed in this part of the mass loss curve may correspond to the simultaneous degradation of more than one constituent (hemicellulose, cellulose, or even lignin). Lignin decomposition starts from around 200 °C [28], but this does not always represent a clear shoulder peak different from hemicellulose and cellulose decomposition peaks. For higher temperatures (T > 350 °C), a slower mass loss corresponding to lignin degradation is observed. Overall, it can be concluded that the major part of pyrolysis conversion occurs at a temperature below 500 °C. The noticeable diminution and/or disappearance of peaks (Fig. 3) for TAS220 and TAS250 in the temperature interval between 30 and 300 °C can be correlated with the differences in moisture and hemicellulose contents. However, taking into account that Van Soest analysis of AS showed a hemicellulose content of 21 %, it can be stated that the second peak observed in the DTG of AS (from 200 °C to 280 °C in Fig. 3), which corresponds to around 30 % of mass loss in the TGA, may correspond not only to hemicellulose degradation but also to the beginning of cellulose or lignin depolymerization. This peak area was significantly reduced in TAS220 and TAS250, which agrees with the almost complete removal of hemicellulose in the torrefied material according to Van Soest analysis (degradation of 85 % and 98.6 % of hemicellulose in TAS200 and TAS250, respectively) [36]. On the other hand, according to some studies in the literature [37], the third peak (from 280 to 360 °C) in the DTG would a priori be mostly attributed to cellulose degradation. However, according to this statement, the third peak in the three solids should have a more similar size, as comparable cellulose contents were found in AS, TAS220 and TAS250 with the Van Soest analysis (Table 2). Hence, the noticeable differences observed in the area of these peaks (Fig. 3) highlight an overlapping of cellulose, hemicellulose and even lignin degradation processes in the temperature range of 220–340 °C [38].

The change in the composition of AS after torrefaction was also observed by ATR FTIR (Fig. 4). In general, the FTIR spectrum of AS changed significantly after torrefaction. The intensity of peaks #1 (wavenumber in the range of 3600–3100 cm^{-1}) and #2 (wavenumber in the range of 3000–2800 cm^{-1}) decreased with the increase of torrefaction temperature, showing the loss of hydroxyl groups by either dehydration reactions or sample drying and the disappearance of alkyl groups in the torrefied AS, respectively. The peak observed at wavenumbers in the range of 1760–1700 cm^{-1} (peak #3), corresponding to the C═O band (typical of acids, esters, aldehydes, and ketones), was especially reduced during the torrefaction of AS. This fact could be correlated with the important release of CO and CO_2 in the generated gas and the collection of acetic acid in the torrefaction liquid during the experiments, which may likely be due to the cleavage of acetyl radicals ($COCH_3$), especially from hemicellulose [28] (see section 3.1.3). Peaks at wavenumbers around 1640–1500 cm^{-1} indicate aromatic links (peak #4), and its intensity in TAS220 and TAS250 was slightly increased compared to the raw AS, which can be correlated with the increase in technical lignin content in the torrefied solids (from 34 to 61–62 wt%, Table 2). Finally, it should also be noted that the reduction of the peaks #6 (~1250 cm^{-1}) and #7 (~1050 cm^{-1}) after torrefaction corresponds to the reduction of hydroxyl groups and ether bonds (C—O—C) in lignin, xylan and cellulose [39].

3.1.3. *Characterization of liquid and gas torrefaction products*

The liquid produced in the torrefaction process mainly comprises water (71 and 60 % on a solvent-free basis at 220 and 250 °C, respectively) and oxygen-containing organic compounds. Hence, water yield reached 19 wt% (at 220 °C) and 24 wt% (at 250 °C) with respect to AS fed, and organic liquid yield (calculated by difference from the total liquid yield) was 8 wt% (at 220 °C) and 16 wt% (at 250 °C) (see Figure S1 in the Supplementary Information Section). The quantification via GC–MS/GC-FID (Table 3) allowed identifying and quantifying around 59–67 % of such mass of organic compounds. Methanol is known to be one of the most abundant organic products in the torrefaction

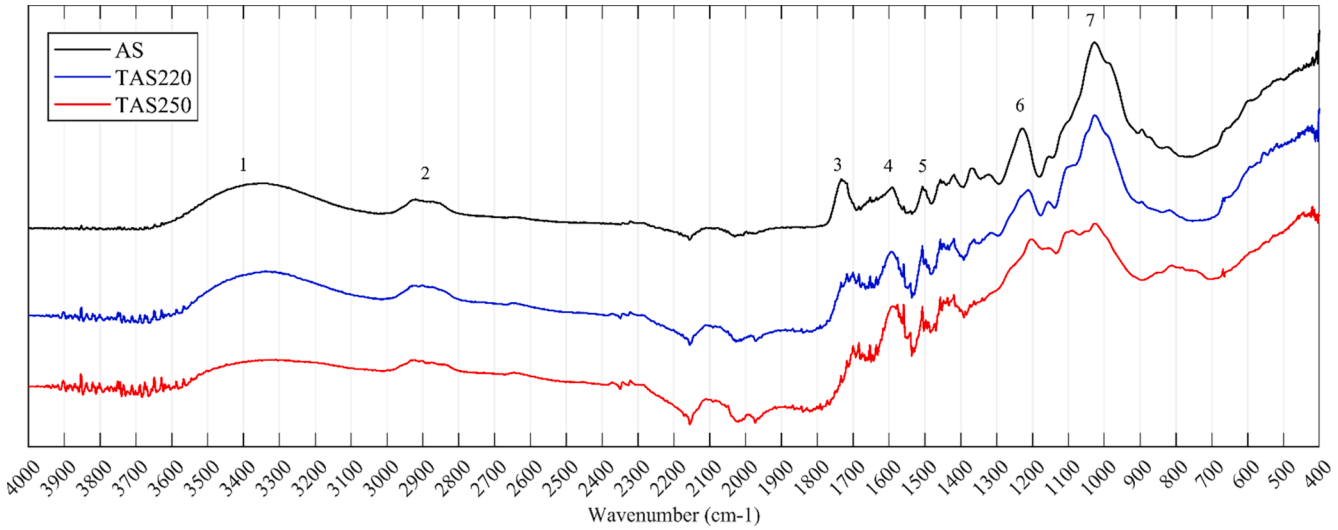

Fig. 4. FTIR spectra of AS before and after torrefaction at 220 and 250 °C.

Table 3
Concentration of organic compounds in the torrefaction liquids (mg/g liquid, quantified by GC-FID).

	Concentration in the torrefaction liquid (mg/g torrefaction liquid)*	
Compound	AS, 220 °C	AS, 250 °C
Furan, tetrahydro-2,5-dimethoxy-	–	1.9
Acetol	6	11
1-Hydroxy-2-butanone	9	11
Acetic acid	146	159
Furfural	14	14
Propanoic acid	5.90	9.3
5-methyl furfuryl	0.500	0.7
2-Furanmethanol	1.7	2.9
2-Cyclopenten-1-one, 2-hydroxy	0.6	1.30
2-Cyclopenten-1-one, 2-hydroxy-3-methyl-	0.6	1.80
Guaiacol	1.5	3.7
Creosol	0.6	2.3
4-Ethylguaiacol	0.5	1.4
Cyclopentanol	–	0.7
Eugenol	–	0.3
4-Vinylguaiacol	0.3	0.6
Phenol, 2,6-dimethoxy-	1.7	4.9
Trans-Isoeugenol	1	1.4
Methoxyeugenol	1	3.4
Benzene, 1,2,3-trimethoxy-5-methyl-	0.5	1.8
Vanillin	0.4	0.6
Guaiacylacetone	–	0.4
Total	191.8	234.4

*Concentration data are expressed on a solvent-free basis.

liquid product [40] due to the degradation of xylan or from the methoxyl groups of uronic acid [41]. Methanol was clearly identified in our chromatograms, but as it had been used as a solvent for recovering the liquid from the condensers, its real production during torrefaction could not be estimated. This fact, together with the presence of oligomeric compounds (with high molecular weight) undetectable by GC [42,43], may fit the remaining fraction of organics that could not be properly explained by GC–MS-FID. Most of the identified organic compounds belong to the families of acids, alcohols, ketones, aldehydes, furans, and phenols (Figure S3 in the Supplementary Information Section). Acids, alcohols, ketones, and furans are typical products of thermal degradation of hemicellulose [44], but they can also be produced during cellulose degradation [41]. More specifically, acids have been found to be produced as soon as the temperature threshold for the thermal decomposition of cellulose (around 270 °C in the case of some woody biomass) is exceeded [45]. On the other hand, the production of phenols is known to result from lignin decomposition.

Table 3 presents the individual GC-FID quantification results of the main compounds identified in the torrefaction liquids. As can be seen, the most abundant compound was acetic acid. Its concentration increased slightly with the torrefaction temperature from 146 to 159 mg/g liquid. Several studies relate the formation of acetic acid in torrefaction with the thermolysis of acetyl radicals linked to the hemicellulose pentosans [28,41]. On the other hand, furfural content, which was also one of the major compounds in the torrefaction liquids, was not affected by the torrefaction temperature. Its formation is related to the dehydration of the xylose unit (hemicellulose component) [46] or to the degradation of cellulose via the dehydration of the formed levoglucosan followed by formaldehyde degradation [47]. Phenols with the highest concentrations in AS torrefaction liquids (essentially methoxy- and dimethoxy- phenols) were derived from coniferyl alcohol (G) and sinapyl alcohol (S), respectively. Temperature promoted the production of most of the identified phenols.

Non-condensable gas was the minority product (by weight) in the torrefaction of AS (Figure S1 in the Supplementary Information Section). On a N_2-free basis, CO_2 (62–65 vol%) and CO (25–30 vol%) were the main gases produced, while CH_4 (6–7 vol%) and H_2 (1 vol%) were detected in smaller percentages. The formation of CO_2 (at this temperature range) is due to the decarboxylation reaction of the carboxyl group in hemicellulose [48,49], while CO is the result of carbonyl, carboxyl and ether groups cracking [49]. Such volumetric concentration data match with the following mass yields calculated with respect to the mass of AS fed: 4–8 wt% for CO_2, 1–2 wt% for CO, 0.2–0.3 wt% for CH_4 and 0.003–0.005 wt% for H_2 (the higher torrefaction temperature, the higher yield).

3.2. Gasification results

3.2.1. Thermodynamic equilibrium model results

As commented, the gasification model described above was run under a wide range of operational conditions (T = 750–1100 °C and S/C = 0–1.1) to determine the ER required for auto-thermal gasification and to evaluate the gas composition once chemical equilibrium was reached for the studied materials (AS, TAS220 and TAS250). Fig. 5 shows the results of these simulations for the raw AS and the torrefied materials at different temperatures and S/C values. The higher the temperature, the higher the ER required for operation. ER for auto-thermal and chemical equilibrium conditions ranges between 30 % and 45 %. Note that the equilibrium calculation in the case of TAS250 has shown lower ER values, especially at the lowest studied temperatures, thus pointing to incomplete solid conversion.

The gas quality is evaluated through the H_2/CO ratio. As expected, the increase of the S/C ratio leads to a higher H_2/CO ratio in all cases, regardless of the temperature evaluated, due to the shift of the water–gas shift reaction (R1), one of the most representative reactions of the gasification process, to the products side. H_2/CO ratio is reduced with increasing temperature (shift of R1 towards left side because of its exothermic character), and this reduction is even more pronounced with the incorporation of steam in the gasification atmosphere due to the enhancement of the water–gas shift reaction. Although higher S/C ratios lead to improved H_2/CO ratios in the producer gas, syngas production (considering this as the joint production of CO and H_2) is not always favored at such conditions, as higher ER is in turn required to reach auto-thermal conditions, which negatively affects the effective use of the raw material due to the conversion of more C into CO_2 (complete combustion, R2).

Water-gas shift (WGS):

$$CO(g) + H_2O(g) \leftrightarrow CO_2(g) + H_2(g)\ \Delta H_{r,\ 298K} = -41.16\ kJ/mol \quad (R1)$$

Oxidation:

$$C(s) + O_2(g) \leftrightarrow CO_2(g)\ \Delta H_{r,\ 298K}\ -393.509\ kJ/mol \quad (R2)$$

Fig. 6 shows the production of CO + H_2 and CO_2 at different temperatures and S/C values for both the raw and torrefied materials. The production of CO + H_2 is enhanced at lower S/C ratios and lower temperatures (both involving lower ER), this occurring at the expense of CO_2 generation. This trend is not observed for TAS250 gasification at the lowest S/C ratios (S/C < 0.5) and temperatures (<900 °C), as a total conversion of the carbonaceous material is not reached. For example, syngas production in AS gasification at 850 °C falls from 1.12 to 1.04 m^3_{STP}/kg when the S/C ratio varies from 0.184 to 1.1, while CO_2 production almost doubles its value (Fig. 6A). A similar effect of S/C is observed for TAS220 (Fig. 6B), even though higher syngas production (1.43 m^3_{STP}/kg TAS220 at S/C of 0.024) and lower CO_2 generation with

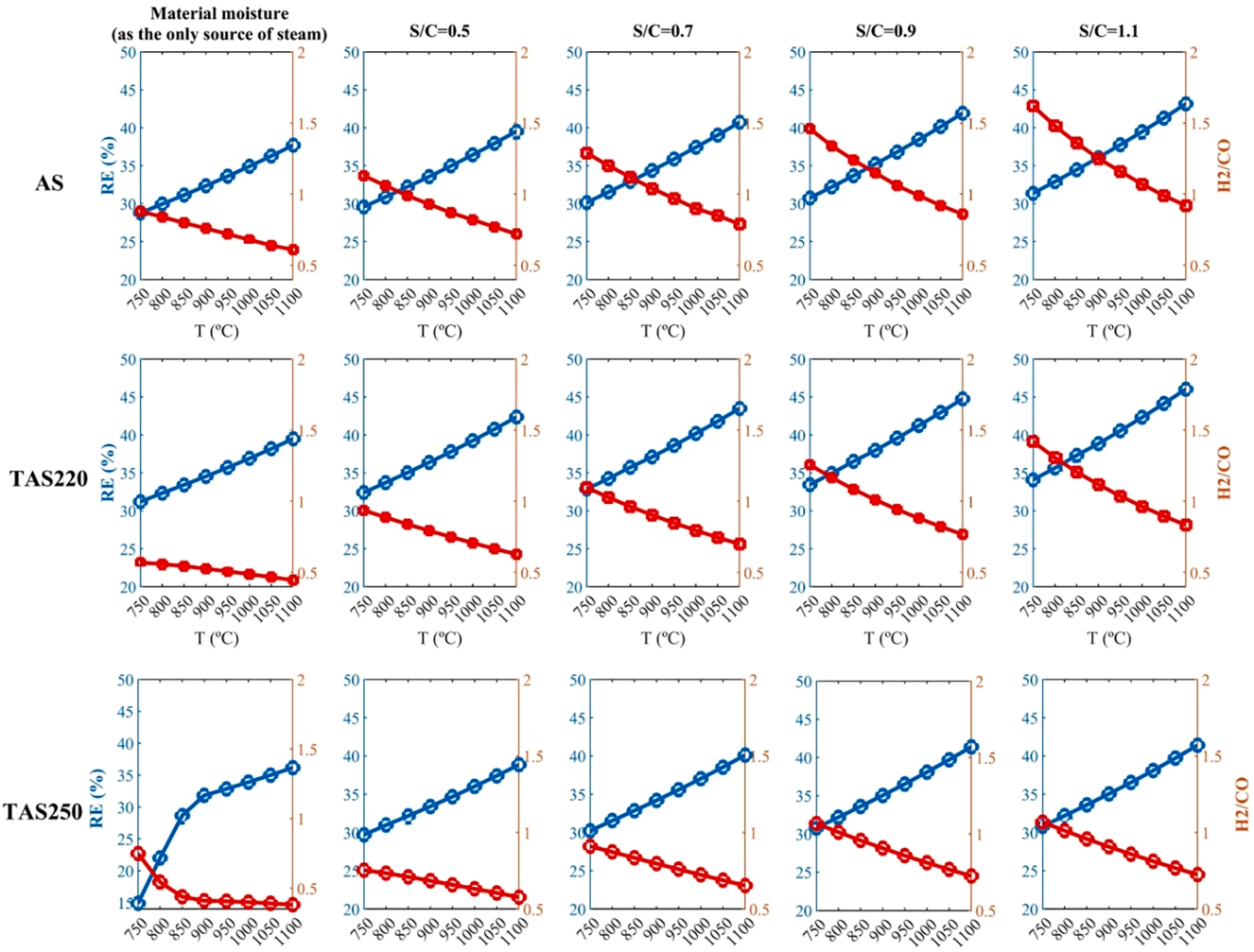

Fig. 5. General view of AS, TAS220 and TAS250 gasification simulation results.

respect to the gasification of raw AS are found. Syngas production is even higher in TAS250 gasification when operating at temperatures above 850 °C and with enough amount of gasifying agent (1.76 m^3_{STP}/kg a S/C = 0.5). Hence, if taking into account the elemental composition of the three materials, it can be concluded that the production of syngas at auto-thermal and equilibrium conditions is favored by lower O/C and H/C ratios in the feedstock (as long as the material can be gasified entirely), not so the H_2/CO ratio in the syngas, which follows the opposite trend.

In summary, these theoretical results from the equilibrium model have pointed out that increasing the S/C ratio is favorable for a higher H_2/CO in the produced gas (Fig. 5), but not for maximizing syngas production (Fig. 6). In addition, too low temperatures could leave behind unconverted solid, especially in the case of torrefied AS. Hence, an intermediate value of S/C ratio (0.5) was set for the gasification experiments, as an agreement between the studied parameters is required to obtain a syngas rich in H_2. Moreover, kinetic aspects usually hinder reaching chemical equilibrium in the process, so tar formation and uncomplete conversion of solid carbon may be expected from real gasification processes. This motivated us to set the gasification temperature for the experiments at a value of 850 °C. Such a combination of temperature and S/C ratio allowed operating at an ER lower than 35 % in all cases, which is favorable for syngas (CO + H_2) production and CO_2 minimization.

3.2.2. Product distribution

Mass balance closed fairly well, between 92 % and 97 %, in all the experiments.

Experimental results for the distribution of gasification products, either from AS or TAS220, are summarized in Table 4. A significant increase in the generation of char (solid product) was observed in the case of TAS220 gasification if compared with the raw AS (10.6 vs 2.3 wt % when using only air and 7.5 vs 1.8 wt% when using air–steam). As the ash content is even lower in the char obtained from TAS220 (Table 4), this noticeable increase in the amount of char could be justified by a reduced reactivity of the raw material after torrefaction. A similar finding has already been reported in the study of Fisher et al. [50] using raw and torrefied short rotation coppice willow. In fact, the carbon content in the remaining solid after TAS220 gasification was found to be significantly higher, while oxygen content was much lower, thus leading to a reduced O/C ratio. Using a mixture of air and steam as the gasifying agent instead of only air slightly decreased the production of char in both cases (AS and TAS220) due to the enhancement of the water–gas reaction (R3) that could further generate CO and H_2, but also due to favored combustion of char (R2), as the addition of steam involves higher ER for auto-thermal operation.

Water-gas reaction:

$$C(s) + H_2O(g) \leftrightarrow CO(g) + H_2(g)\ \Delta H_{r,\ 298K} = 131.30\ kJ/mol \quad (R3)$$

The yield of liquid product (including tar and condensed water) was found to increase when adding steam as gasifying agent (from 22 to 30 wt% for AS gasification and from 17.9 to 34 wt% for TAS220). Such a rough increase in the liquid yield may not necessarily mean a higher tar

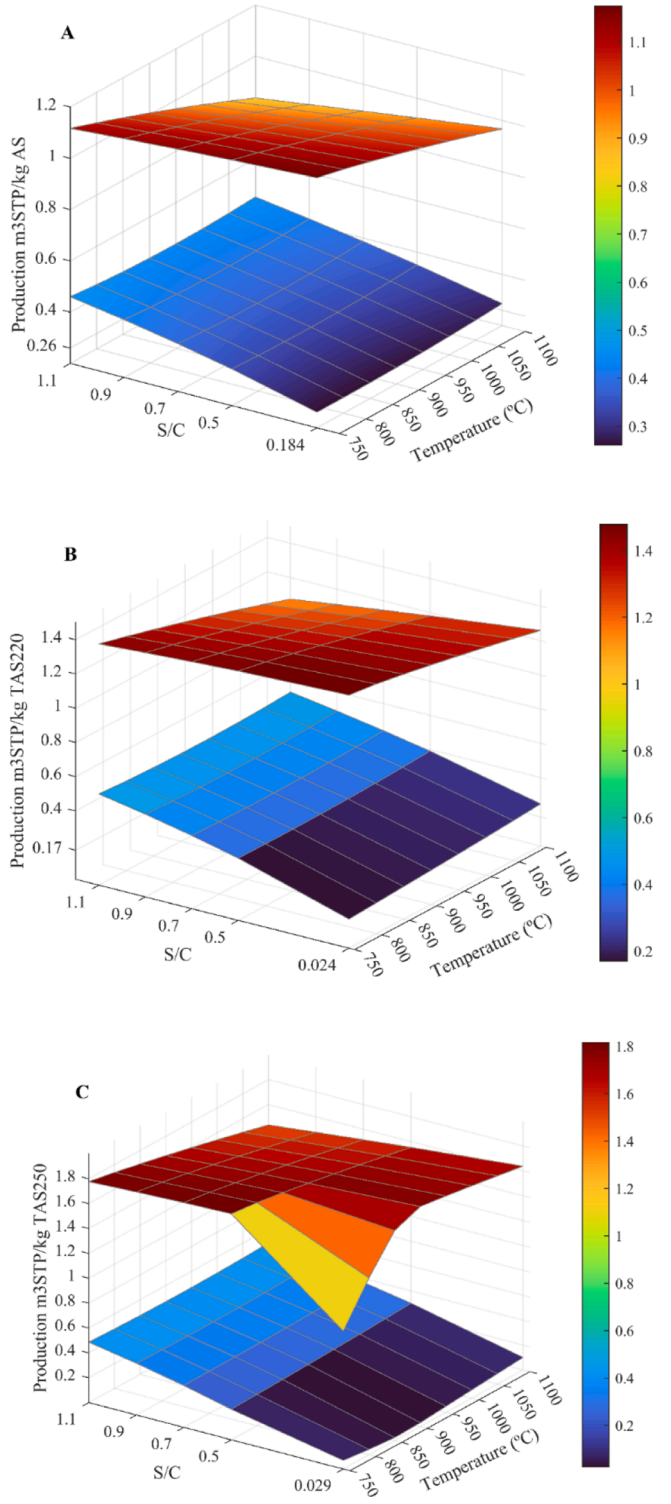

Fig. 6. Theoretical production of CO + H_2 (red surface) and CO_2 (blue surface) at different temperatures and S/C ratios for AS (A), TAS220 (B) and TAS250 (C) gasification.

formation (see section 3.2.4), as un-converted or produced water is also included in this yield.

On the other hand, the fact of having "strange" gas yields above 100 % is only a matter of the calculation basis (the reference is only biomass).

The volumetric gas production is usually defined in the gasification studies as a more representative factor of syngas generation. As shown in

Table 4
Experimental results from the gasification at 850 °C of AS and TAS220.

Run Material	1 & 2 AS	3 & 4 AS	5 TAS220	6 TAS220
Reaction medium	Air	Air-steam	Air	Air-steam
Product yield (wt. %)				
Char	2.3 ± 0.4	1.8 ± 0.6	10.6	7.5
Liquid (tar + water)	22 ± 1	30.24 ± 0.02	17.9	34
Gas (N_2 free basis)	135 ± 2	133 ± 7	138	148
Syngas composition (vol. %)				
H_2	9.4 ± 0.9	11 ± 2	6.9	9.4
CO	14 ± 1	12 ± 1	11	10
CO_2	17.3 ± 0.2	18.2 ± 0.3	17	18
CH_4	0.3	3.9 ± 0.4	3.1	3.0
C_2H_6	4.0 ± 0.2	0.12 ± 0.03	0.1	0.1
C_2H_4	0.14 ± 0.02	0.9 ± 0.1	0.6	0.6
C_2H_2	0.9 ± 0.1	0.08 ± 0.01	0.1	0.03
H_2S	0.07 ± 0.05	0.10 ± 0.01	0.01	0.1
N_2	0.1 ± 0.05	54 ± 3	62	59
	54 ± 2			
H_2/CO ratio	0.69 ± 0.04	0.90 ± 0.04	0.64	0.94
CO/CO_2 ratio	0.81 ± 0.04	0.7 ± 0.1	0.63	0.57
Cold gas efficiency (%)	66 ± 4	66 ± 9	45.3 (37)	48.7 (40)
LHV_{gas} (MJ/m^3_{STP})	4.7 ± 0.3	4.5 ± 0.5	3.6	3.6
Gas production(m^3_{STP}/kg material)	2.37 ± 0.01	2.4 ± 0.1	2.7 (1.8)	2.9 (1.9)
Gas production N_2-free basis (m^3_{STP}/kg material)	1.1 ± 0.4	1.1 ± 0.1	1.1 (0.7)	1.2 (0.8)
Carbon yield to the gas phase (%)	100 ± 2	97 ± 7	79	83
Concentration of tar in syngas, g/m^3_{STP} (GC–MS)	0.7 ± 0.1	0.6 ± 0.1	0.7	0.3
Char characterization (elemental analysis and ash content, wt. %)				
C	83 ± 7	79.9	92.8	92.6
H	2 ± 1	1.3	0.9	1.1
N	0.7 ± 0.1	0.8	1	0.9
O	8.1	11.1	2.9	2.8
Ash	6.2 ± 0.1	6.9	2.4	2.5

The values shown in brackets for TAS220 gasification represent the analogous results obtained if considering for the calculations the original amount of AS that was torrefied instead of the amount of TAS220 that was gasified.

Table 4, this factor has shown values of around 2.4 m^3_{STP}/kg for AS, while increased up to 2.7–2.9 m^3_{STP}/kg for TAS220. These gas production data include N_2 coming from air and, as TAS220 gasification involved highest values of ER (see Table 1), it means that N_2 feeding was also greater. By considering a N_2-free basis for gas production, such differences between the raw AS and the torrefied material practically disappear (1.1–1.2 m^3_{STP}/kg material). As expected, if gas production in TAS220 gasification is calculated with respect to the original amount of AS previously torrefied, it falls by around 25 % (0.7–0.8 m^3_{STP}/kg AS). The N_2-free gas produced in the torrefaction stage (0.08 m^3_{STP}/kg AS) does not offset such a difference.

3.2.3. Syngas composition and properties

Besides the reactions previously commented, a wide range of exothermic and endothermic reactions occur during the different stages

taking place in the gasification process:

Partial oxidation:

$$C(s) + 1/2O_2(g) \leftrightarrow CO(g)\ \Delta H_{r,\ 298K} = -110.53\ kJ/mol \quad (R4)$$

Boudouard:

$$C(s) + CO_2(g) \leftrightarrow 2CO(g)\ \Delta H_{r,\ 298K} = 172.45\ kJ/mol \quad (R5)$$

Methanation:

$$C(s) + 2H_2(g) \leftrightarrow CH_4(g)\ \Delta H_{r,\ 298K} = -74.85\ kJ/mol \quad (R6)$$

Steam reforming:

$$C_xH_y(g) + xH_2O(g) \leftrightarrow xCO(g) + (y/2 + x)\ H_2(g)\ \Delta H > 0 \quad (R7)$$

Dry reforming:

$$C_xH_y(g) + xCO_2(g) \leftrightarrow 2xCO(g) + (y/2)\ H_2(g)\ \Delta H > 0 \quad (R8)$$

Cracking:

$$C_xH_y(g) \leftrightarrow xC(s) + (y/2)\ H_2(g)\ \Delta H > 0 \quad (R9)$$

According to the results exposed in Table 4, the gasification of AS and TAS220 produced significant amounts of H_2, CO, CO_2, light hydrocarbons (predominantly CH_4) and H_2S (detected and quantified by micro-GC). As predicted by the equilibrium calculations, the experimental data confirmed that adding steam to the gasifying agent improved the quality of the gas. H_2 concentration was increased from 9.7 % vol. to 11 % vol. when adding steam (S/C = 0.5) in the case of AS gasification. Lower H_2 concentrations were obtained in the case of TAS gasification: 6.9 % vol. when gasifying with only air and 9.4 % vol. at S/C = 0.5. The opposite behavior was found for CO concentration, which decreased when steam was added. This reverse relation between H_2 and CO concentrations directly affects the H_2/CO ratio, which was enhanced by adding steam from 0.69 to 0.9 in the case of AS and from 0.64 to 0.94 for TAS220. Therefore, the torrefaction of AS did not further improve the H_2/CO ratio in the syngas. These H_2/CO values were greater than those reported in the literature for the gasification of similar materials, such as almond shells gasification in an updraft reactor at 850 °C, for which the H_2/CO ratio ranged between 0.46 (S/C = 0) and 0.75 (S/C = 0.2) [11]. The torrefaction stage neither played an important role in the production of CO_2 during the subsequent gasification, as it was maintained around 17 % vol. in all cases when gasifying with only air. A slight increase was observed when adding steam, which could boost either the water–gas shift reaction or combustion reactions because of the simultaneous increase of the ER (needed to keep the reaction at 850 °C). As expected, the production of light hydrocarbons during gasification was significantly affected by the previous torrefaction stage.

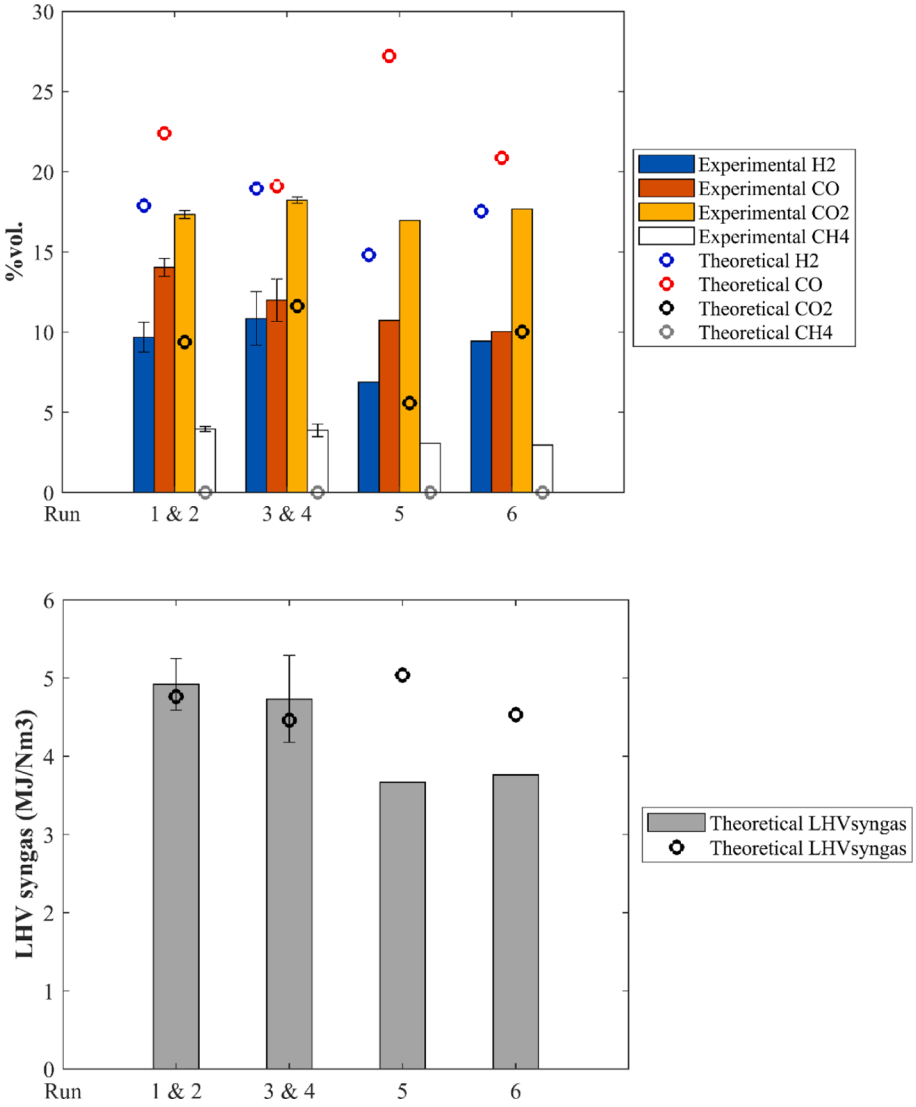

Fig. 7. Theoretical and experimental concentrations of CO, H_2, CO_2 and CH_4 (% vol.) in the gasification gas and corresponding LHVs.

The concentration of CH_4 was around 25 % lower in TAS220 gas. This fact seems to be directly related to the volatile matter released during the torrefaction process. As a result, the volatile matter content in the raw material was significantly reduced: 75 wt% in AS vs 69 wt% in TAS220. A similar trend was observed by Strandberg [51], who compared the gasification of raw and torrefied woody residues. As mentioned in that work, the main reason for CH_4 presence in the gasification syngas is an unconverted fraction of pyrolysis products coming from the volatile components in the raw biomass. It is to highlight that the CH_4 content was not affected by the composition of the gasifying agent for both materials (no significant effect of steam addition was observed).

Fig. 7 compares the experimental gas composition obtained at the different operating conditions with the theoretical data predicted by the equilibrium model (only including the four main gas products). Theoretical and experimental data are noticeably different. The equilibrium calculations predicted higher concentrations of H_2 and CO (approximately double) than those experimentally obtained in the lab setup, while the experimental content of CO_2 almost doubled the simulation prediction in some cases. The model expected only traces of CH_4 (<0.01 % vol.), while real concentrations obtained in the gasification experiments were between 3 and 4 % vol. This divergence between the theoretical and experimental data means that the equilibrium was not reached during the experiments at these operational conditions.

Besides composition, other important characteristics of the produced syngas, such as its lower heating value (LHV_{gas}), the carbon conversion to the gas phase and the cold gas efficiency are also included in Table 4. The addition of steam to the gasification atmosphere did not significantly affect the LHV of the gas obtained from any of the two materials gasified. Typical values between 3 and 5 MJ/m^3 are reported in the literature for the LHV of the syngas obtained in the air gasification of many lignocellulosic materials (woody, herbaceous or fruit-shells [17,52,53]). For instance, in the study of Kulkarni et al. [17], the LHV of the syngas was 5.2 MJ/Nm^3 for pine gasification. For walnut and pistachio shells, the study of Karatas and Akgun [52] reported LHV values of up to 5 MJ/m^3 at lower ER values. The ER plays a significant role in the LHV of the gas because of the N_2 dilution effect. However, significant differences were found in the LHV_{gas} when comparing the gas from AS and TAS220, as it was reduced by around 1 MJ/m^3_{STP} when feeding the torrefied material. This reduction may be related to the lower content of combustible gases such as CH_4, H_2 and CO and the increased fraction of N_2 in the syngas from TAS220. A similar trend was observed in other work in the literature for the gasification of raw and torrefied switchgrass (at 230 and 270 °C), for which the LHV_{gas} decreased in 0.4 and 0.6 MJ/m^3, respectively [53]. Kulkarni et al. reported a decrease of up to 0.7 MJ/Nm^3 in LHV_{gas} after the gasification of torrefied pine [17].

As shown in Fig. 7, the equilibrium-based model used to simulate the gasification of AS and TAS220, either with air or air–steam, predicted minor differences between the values of LHV_{gas} obtained from both materials, all of them ranging between 4.5 and 5.1 MJ/m^3_{STP}. The experimental values of LHV_{gas} obtained in the case of AS gasification were quite similar to the model estimations, while in the case of TAS220, the theoretical values were higher. The theoretical model does not consider the nature of the chemical bonds in the original materials. However, the kinetics of the gasification process has been experimentally proved to be affected by the chemical transformations occurring in the previous torrefaction stage (as shown by the higher char yield obtained in the gasification of TAS220), which in turn results in important differences in the composition and the LHV of the syngas.

The LHV of the syngas directly affects the cold gas efficiency (Equation (3)). The gasification of AS showed a cold gas efficiency higher than 60 %, while in the case of TAS220 gasification, it reached 49 % as the maximum value. This difference is explained by the lower energy density in the gas from TAS220. The cold gas efficiency for the gasification of the torrefied material is even lower (37–40 %) if considering the initial amount of AS that was torrefied as the calculation reference. However, gas from torrefaction (LHV = 0.6 MJ/m^3_{STP}) could also be considered to calculate a global cold gas efficiency for the two-stages process, obtaining a result of 40–43 %. From this point of view, the two-stages process is less efficient than the direct gasification of the raw AS.

Another interesting parameter to assess the gasification performance is the carbon yield to the gas phase, which is the ratio between the mass of carbon contained in the syngas and the mass of carbon in the material fed (fraction of carbon converted to gaseous compounds). At equilibrium conditions, this ratio was estimated to be 100 % in all cases. However, lower values were obtained experimentally (Table 4), especially for TAS220 (79 and 83 %). This difference points to slower kinetics for the gasification of the torrefied material.

3.2.4. Production of tar

The production of tar in the gasification runs was quantified by GC–MS-FID analysis. Table 4 exposes the concentration of tar in the produced syngas, which was quite similar in most cases (between 0.6 and 0.7 g/m^3_{STP}), except when gasifying TAS220 at a S/C ratio of 0.5, for which a decrease of 50 % was observed. This was also confirmed in terms of tar yield with respect to the material fed, which ranged around 1.5–1.7 g/kg in the case of AS and dropped from 1.9 to 0.9 g/kg in the case of TAS220 gasification (Table 5). Kulkarni et al. [17] observed that the gasification of torrefied pine (at a temperature of 935 °C and ER of 25 %) reduced by half the production of tar compared to the original material (from 8 to 3.9 g/kg dried biomass). In the present work, we used calcined dolomite as bed material, which has been proved to be efficient in tar cracking at analogous operating conditions (temperature and use of steam) [29], which might be the reason for such low values of tar production.

Tar is mainly composed of polycyclic aromatic hydrocarbons (PAHs). Table 5 summarizes the composition of the identified tar (mass fractions), including 11 different PAHs detected in the condensed liquids. As shown, naphthalene, acenaphthylene and phenanthrene were the main tar compounds, accounting for 55–65 % of the produced tar. The formation of these aromatic tar species without substituent groups is favored in the temperature range of 750 to 900 °C [54]. According to Devi et al., such types of aromatics are considered the most challenging tar fraction to destroy because of their stability [54]. Steam addition to

Table 5
Production of tar in the gasification experiments and composition of tar samples (GC/MS/FID).

Run	1 & 2	3 & 4	5	6
Material, S/C	AS, 0.184	AS, 0.5	TAS220, 0.024	TAS220, 0.5
Production of tar (g/kg material)	1.7 ± 0.2	1.5 ± 0.2	1.9	0.9
Tar composition (wt.%)				
Naphthalene	42 ± 6	35 ± 6	43.2	34.9
Acenaphthylene	13 ± 2	11 ± 2	12.9	12.1
Acenaphthene	2.1 ± 0.1	2.9 ± 0.1	2.6	3.9
Fluorene	5.4 ± 0.4	5.7 ± 0.6	6.1	6.5
Phenanthrene	9 ± 1	9 ± 2	9.2	10.3
Anthracene	3.7 ± 0.3	4.2 ± 0.5	4.1	4.9
Fluoranthene	3.8 ± 0.4	4.3 ± 0.5	4.2	5.2
Pyrene	3.6 ± 0.4	4.2 ± 0.6	4.2	5.1
Benz[*a*]anthracene	3.5 ± 0.08	5.0 ± 0.4	4.7	5.9
Chrysene	3.5 ± 0.1	4.8 ± 0.3	4.5	5.8
Benzo[*b*]fluoranthene	3.0 ± 0.2	4.5 ± 0.3	4.2	5.4

the gasification atmosphere contributed to decreasing the individual production of these PAHs. For example, naphthalene yield dropped from 0.8 to 0.6 g/kg in the case of AS and from 0.8 to 0.3 g/kg in the case of TAS220 by increasing the S/C ratio up to 0.5. Steam reforming reactions (R7) may be involved in such observed reduction [55]. In summary, tar production during the gasification of AS or TAS220 with air was hardly affected by the torrefaction stage previously undergone by the solid, while a reduction in tar production was observed when adding steam to the TAS220 gasification atmosphere. However, tar composition was hardly impacted by the torrefaction stage, as the same PAHs (naphthalene, acenaphthylene and phenanthrene) were identified as the majority ones.

4. Conclusions

The torrefaction of argan nutshells (AS) has been experimentally studied at lab-scale as a potential process to improve its properties as fuel. This biomass showed a very reactive behavior even at moderate torrefaction temperatures (220–250 °C). Compared to the raw material, the torrefied solid product (yield between 49.7 and 65.8 wt%) was richer in fixed carbon and showed a lower O/C ratio and an important increase in the HHV (from 18.6 MJ/kg for the argan nutshells up to 27 MJ/kg for the material torrefied at 250 °C). Hemicellulose was almost totally removed from argan nutshells after torrefaction.

The gasification experimental study (planned for operating at auto-thermal conditions), as well as the chemical equilibrium theoretical model implemented for such auto-thermal operation, revealed that adding steam to the gasification atmosphere has a beneficial effect on the syngas composition by improving its H_2/CO ratio. The theoretical model pointed out that the lower O/C and H/C ratios found in the torrefied solid (TAS220) should leave behind a higher production of syngas ($CO + H_2$) and a lower H_2/CO ratio in the syngas, but this result was not observed experimentally, pointing that chemical equilibrium was not achieved in the experimental runs. The H_2/CO ratio was slightly higher for the torrefied material (0.94 for TAS220 vs 0.9 for AS), while the lower heating value of the gas from TAS220 was reduced mainly because of its lower CH_4 content (4.7 MJ/m^3_{STP} for AS gasification vs 3.6 MJ/m^3_{STP} for TAS220 gasification).

Tar reduction was one of the major expected advantages of including torrefaction as a pretreatment step before argan nutshells gasification. However, in the presence of dolomite, tar reduction was only slightly observed when adding steam into the gasification atmosphere (0.7 g/m^3_{STP} for AS gasification vs 0.3 g/m^3_{STP} for TAS220). On the other hand, argan nutshells turned less reactive after torrefaction, thus resulting in higher char formation and lower conversion of carbon to the gas phase, also with a lower CO/CO_2 distribution ratio. Hence, torrefaction as a pretreatment stage has not brought many benefits in terms of syngas production and quality for the gasification of argan nutshells.

CRediT authorship contribution statement

Zainab Afailal: Methodology, Investigation, Writing – original draft. **Noemí Gil-lalaguna:** Methodology, Investigation, Writing – review & editing. **Isabel Fonts:** Writing – review & editing. **Alberto Gonzalo:** Writing – review & editing, Project administration. **Jesús Arauzo:** Supervision, Project administration, Funding acquisition. **José Luis Sánchez:** Writing – review & editing, Supervision, Funding acquisition.

Declaration of Competing Interest

The authors declare that they have no known competing financial interests or personal relationships that could have appeared to influence the work reported in this paper.

Data availability

E-supplementary data of this work can be found in the paper's online version.

Acknowledgments

The authors express their gratitude to Agencia Estatal de Investigación in Spain (project PID2020-114936RB-I00) and Aragón Government (Research Group Ref. T22_20R) for providing frame support for this work. I. Fonts acknowledges the MINECO, European Social Fund, AEI and Unizar for the post-doctoral contract awarded (RYC2020-030593-I).

Appendix A. Supplementary data

Supplementary data to this article can be found online at https://doi.org/10.1016/j.fuel.2022.125970.

References

[1] Huber GW, Iborra S, Corma A. Synthesis of Transportation Fuels from Biomass: Chemistry, Catalysts, and Engineering. Chem Rev 2006;106(9):4044–98. https://doi.org/10.1021/cr068360d.
[2] Dahbi M, Kiso M, Kubota K, Horiba T, Chafik T, Hida K, et al. Synthesis of hard carbon from argan shells for Na-ion batteries. J Mater Chem A 2017;5(20):9917–28. https://doi.org/10.1039/c7ta01394a.
[3] Rahib Y, Boushaki T, Sarh B, Chaoufi J, Ihlal A, Bonammy S, et al. Combustion Analysis of Fixed Beds of Argan Nut Shell (ANS) Biomass in a Batch Type Reactor. In: in 2019 7th International Renewable and Sustainable Energy Conference (IRSEC); 2019. https://doi.org/10.1109/irsec48032.2019.9078217.
[4] Rahib Y, Elorf A, Sarh B, Ezahri M, Rahib Y, Bonnamy S. Experimental Analysis on Thermal Characteristics of Argan Nut Shell (ANS) Biomass as a Green Energy Resource. International Journal of Renewable Energy Research 2019;9(4):1606–15.
[5] Afailal Z, Gil-Lalaguna N, Torrijos MT, Gonzalo A, Arauzo J, Sánchez JL. Antioxidant Additives Produced from Argan Shell Lignin Depolymerization. Energy Fuels 2021;35(21):17149–66. https://doi.org/10.1021/acs.energyfuels.1c01705.
[6] Demirbaş A. Calculation of higher heating values of biomass fuels. Fuel 1997;76(5):431–4. https://doi.org/10.1016/S0016-2361(97)85520-2.
[7] Rapagnà S, Latif A. Steam gasification of almond shells in a fluidised bed reactor: the influence of temperature and particle size on product yield and distribution. Biomass Bioenergy 1997;12(4):281–8.
[8] Roger M. Rowell R.P., Mandla A. Tshabalala. Cell Wall Chemistry. In Handbook of Wood Chemistry and Wood Composites, Rowell, R.M., Editor CRC Press (2012). p.
[9] Nguyen NM, Alobaid F, May J, Peters J, Epple B. Experimental study on steam gasification of torrefied woodchips in a bubbling fluidized bed reactor. Energy 2020;202:117744. https://doi.org/10.1016/j.energy.2020.117744.
[10] Ahrenfeldt J, Knoef H. GasNet. Netherlands: Handbook biomass gasificationBTG Biomass Technology Group Enschede; 2005.
[11] Cerone N, Zimbardi F, Contuzzi L, Baleta J, Cerinski D, Skvorčinskienė R. Experimental investigation of syngas composition variation along updraft fixed bed gasifier. Energy Convers Manage 2020;221:113116. https://doi.org/10.1016/j.enconman.2020.113116.
[12] Dayton DC, Turk B, Gupta R. Syngas Cleanup, Conditioning, and Utilization. In Thermochemical Processing of. Biomass 2019:125–74.
[13] P.L. Spath D.C.D., ed. Preliminary Screening – Technical and economic assessment of synthesis gas to fuels and chemicals with emphasis on the potential for biomass-derived syngas. ed. report, T.2003: United States. doi: 10.2172/15006100.
[14] Gil-Lalaguna N, Sánchez JL, Murillo MB, Rodríguez E, Gea G. Air–steam gasification of sewage sludge in a fluidized bed. Influence of some operating conditions. Chem Eng J 2014;248:373–82. https://doi.org/10.1016/j.cej.2014.03.055.
[15] Cerone N, Zimbardi F, Villone A, Strjiugas N, Kiyikci EG. Gasification of Wood and Torrefied Wood with Air, Oxygen, and Steam in a Fixed-Bed Pilot Plant. Energy Fuels 2016;30(5):4034–43. https://doi.org/10.1021/acs.energyfuels.6b00126.
[16] Chen W-H, Chen C-J, Hung C-I, Shen C-H, Hsu H-W. A comparison of gasification phenomena among raw biomass, torrefied biomass and coal in an entrained-flow reactor. Appl Energy 2013;112:421–30. https://doi.org/10.1016/j.apenergy.2013.01.034.
[17] Kulkarni A, Baker R, Abdoulmomine N, Adhikari S, Bhavnani S. Experimental study of torrefied pine as a gasification fuel using a bubbling fluidized bed gasifier. Renewable Energy 2016;93:460–8. https://doi.org/10.1016/j.renene.2016.03.006.
[18] Li M-F, Chen L-X, Li X, Chen C-Z, Lai Y-C, Xiao X, et al. Evaluation of the structure and fuel properties of lignocelluloses through carbon dioxide torrefaction. Energy Convers Manage 2016;119:463–72. https://doi.org/10.1016/j.enconman.2016.04.064.

[19] Rahib Y, Boushaki T, Sarh B, Chaoufi J. Combustion and pollutant emission characteristics of argan nut shell (ANS) biomass. Fuel Process Technol 2021;213:106665. https://doi.org/10.1016/j.fuproc.2020.106665.
[20] Cazaña F, Afailal Z, González-Martín M, Sánchez JL, Latorre N, Romeo E, et al. Hydrogen and CNT Production by Methane Cracking Using Ni–Cu and Co–Cu Catalysts Supported on Argan-Derived Carbon. ChemEngineering 2022;6(4):47.
[21] Barco-Burgos J, Carles-Bruno J, Eicker U, Saldana-Robles AL, Alcántar-Camarena V. Hydrogen-rich syngas production from palm kernel shells (PKS) biomass on a downdraft allothermal gasifier using steam as a gasifying agent. Energy Convers Manage 2021;245:114592. https://doi.org/10.1016/j.enconman.2021.114592.
[22] Zubair YA, Rao SM, Muchtar A, Anwar SS, Daud RW, W.. Effects of temperature on the chemical composition of tars produced from the gasification of coconut and palm kernel shells using downdraft fixed-bed reactor. Fuel 2020;265:116910. https://doi.org/10.1016/j.fuel.2019.116910.
[23] Menon SD, Sampath K, Kaarthik SS. Feasibility studies of coconut shells biomass for downdraft gasification. Mater Today: Proc 2021;44:3133–7. https://doi.org/10.1016/j.matpr.2021.02.813.
[24] Yahaya AZ, Somalu MR, Muchtar A, Sulaiman SA, Wan Daud WR. Effect of particle size and temperature on gasification performance of coconut and palm kernel shells in downdraft fixed-bed reactor. Energy 2019;175:931–40. https://doi.org/10.1016/j.energy.2019.03.138.
[25] Macrì D, Catizzone E, Molino A, Migliori M. Supercritical water gasification of biomass and agro-food residues: Energy assessment from modelling approach. Renewable Energy 2020;150:624–36. https://doi.org/10.1016/j.renene.2019.12.147.
[26] Godin B, Agneessens R, Gofflot S, Lamaudière S, Sinnaeve G, Gerin PA, et al. Revue bibliographique sur les méthodes d'analyse des polysaccharides structuraux des biomasses lignocellulosiques. Biotechnologie, Agronomie, Société et Environnement 2011;15(1):165–82.
[27] Scanlon JT, Willis DE. Calculation of Flame Ionization Detector Relative Response Factors Using the Effective Carbon Number Concept. J Chromatogr Sci 1985;23(8):333–40. https://doi.org/10.1093/chromsci/23.8.333.
[28] Nunes LJR, De Oliveira Matias JC, Da Silva CJP. Chapter 3 - Biomass Torrefaction Process. In: Nunes LJR, De Oliveira Matias JC, Da Silva Catalão JP, editors. Torrefaction of Biomass for Energy Applications. Academic Press; 2018. p. 89–124.
[29] Berrueco C, Montané D, Matas GB, del Alamo G. Effect of temperature and dolomite on tar formation during gasification of torrefied biomass in a pressurized fluidized bed. Energy 2014;66:849–59. https://doi.org/10.1016/j.energy.2013.12.035.
[30] Gil-Lalaguna N, Afailal Z, Aznar M, Fonts I. Exploring the sustainable production of ammonia by recycling N and H in biological residues: Evolution of fuel-N during glutamic acid gasification. J Cleaner Prod 2021;282:124417. https://doi.org/10.1016/j.jclepro.2020.124417.
[31] Boonstra M., A two-stage thermal modification of wood, (2008), Editor˚Editors, Ghent University.
[32] Grigiante M, Antolini D. Experimental Results of Mass and Energy Yield Referred to Different Torrefaction Pathways. Waste Biomass Valorization 2014;5(1):11–7. https://doi.org/10.1007/s12649-013-9205-3.
[33] Brachi P, Riianova E, Miccio M, Miccio F, Ruoppolo G, Chirone R. Valorization of Sugar Beet Pulp via Torrefaction with a Focus on the Effect of the Preliminary Extraction of Pectins. Energy Fuels 2017;31(9):9595–604. https://doi.org/10.1021/acs.energyfuels.7b01766.
[34] Asadullah M, Adi AM, Suhada N, Malek NH, Saringat MI, Azdarpour A. Optimization of palm kernel shell torrefaction to produce energy densified bio-coal. Energy Convers Manage 2014;88:1086–93. https://doi.org/10.1016/j.enconman.2014.04.071.
[35] Brachi P, Chirone R, Miccio M, Ruoppolo G. Fluidized Bed Torrefaction of Commercial Wood Pellets: Process Performance and Solid Product Quality. Energy Fuels 2018;32(9):9459–69. https://doi.org/10.1021/acs.energyfuels.8b01519.
[36] Kizuka R, Ishii K, Ochiai S, Sato M, Yamada A, Nishimiya K. Improvement of Biomass Fuel Properties for Rice Straw Pellets Using Torrefaction and Mixing with Wood Chips. Waste Biomass Valorization 2021;12(6):3417–29.
[37] Chen W-H, Kuo P-C. A study on torrefaction of various biomass materials and its impact on lignocellulosic structure simulated by a thermogravimetry. Energy 2010;35(6):2580–6. https://doi.org/10.1016/j.energy.2010.02.054.
[38] Di Blasi C. Modeling chemical and physical processes of wood and biomass pyrolysis. Prog Energy Combust Sci 2008;34(1):47–90. https://doi.org/10.1016/j.pecs.2006.12.001.
[39] Shi J, Xing D, Lia J. FTIR Studies of the Changes in Wood Chemistry from Wood Forming Tissue under Inclined Treatment. Energy Procedia 2012;16:758–62. https://doi.org/10.1016/j.egypro.2012.01.122.
[40] Medic D, Darr M, Shah A, Potter B, Zimmerman J. Effects of torrefaction process parameters on biomass feedstock upgrading. Fuel 2012;91(1):147–54. https://doi.org/10.1016/j.fuel.2011.07.019.
[41] Demirbaş A. Mechanisms of liquefaction and pyrolysis reactions of biomass. Energy Convers Manage 2000;41(6):633–46. https://doi.org/10.1016/S0196-8904(99)00130-2.
[42] Fonts I, Atienza-Martínez M, Carstensen H-H, Benés M, Pinheiro Pires AP, Garcia-Perez M, et al. Thermodynamic and Physical Property Estimation of Compounds Derived from the Fast Pyrolysis of Lignocellulosic Materials. Energy Fuels 2021;35(21):17114–37. https://doi.org/10.1021/acs.energyfuels.1c01709.
[43] Pinheiro Pires AP, Arauzo J, Fonts I, Domine ME, Fernández AA, Garcia-Perez ME, et al. Challenges and Opportunities for Bio-oil Refining: A Review. Energy Fuels 2019;33(6):4683–720. https://doi.org/10.1021/acs.energyfuels.9b00039.
[44] Zheng A, Zhao Z, Chang S, Huang Z, He F, Li H. Effect of Torrefaction Temperature on Product Distribution from Two-Staged Pyrolysis of Biomass. Energy Fuels 2012;26(5):2968–74. https://doi.org/10.1021/ef201872y.
[45] Melkior T, Jacob S, Gerbaud G, Hediger S, Le Pape L, Bonnefois L, et al. NMR analysis of the transformation of wood constituents by torrefaction. Fuel 2012;92(1):271–80. https://doi.org/10.1016/j.fuel.2011.06.042.
[46] Demirbas A. Pyrolysis of ground beech wood in irregular heating rate conditions. J Anal Appl Pyrol 2005;73(1):39–43. https://doi.org/10.1016/j.jaap.2004.04.002.
[47] Van der Stelt MJC. Chemistry and reaction kinetics of biowaste torrefaction 2011. https://doi.org/10.6100/IR695294.
[48] Atienza-Martínez M, Mastral JF, Ábrego J, Ceamanos J, Gea G. Sewage Sludge Torrefaction in an Auger Reactor. Energy Fuels 2015;29(1):160–70. https://doi.org/10.1021/ef501425h.
[49] Yang H, Yan R, Chen H, Lee DH, Zheng C. Characteristics of hemicellulose, cellulose and lignin pyrolysis. Fuel 2007;86(12):1781–8. https://doi.org/10.1016/j.fuel.2006.12.013.
[50] Fisher EM, Dupont C, Darvell LI, Commandré JM, Saddawi A, Jones JM, et al. Combustion and gasification characteristics of chars from raw and torrefied biomass. Bioresour Technol 2012;119:157–65. https://doi.org/10.1016/j.biortech.2012.05.109.
[51] Strandberg M. From torrefaction to gasification Pilot scale studies for upgrading of biomass. Department of Applied Physics and Electronics. Umeå University; 2015. Vol. Doctoral Thesis.
[52] Karatas H, Akgun F. Experimental results of gasification of walnut shell and pistachio shell in a bubbling fluidized bed gasifier under air and steam atmospheres. Fuel 2018;214:285–92. https://doi.org/10.1016/j.fuel.2017.10.061.
[53] Sarkar M, Kumar A, Tumuluru JS, Patil KN, Bellmer DD. Gasification performance of switchgrass pretreated with torrefaction and densification. Appl Energy 2014;127:194–201. https://doi.org/10.1016/j.apenergy.2014.04.027.
[54] Devi L, Ptasinski KJ, Janssen FJJG. Pretreated olivine as tar removal catalyst for biomass gasifiers: investigation using naphthalene as model biomass tar. Fuel Process Technol 2005;86(6):707–30. https://doi.org/10.1016/j.fuproc.2004.07.001.
[55] Yu H, Zhang Z, Li Z, Chen D. Characteristics of tar formation during cellulose, hemicellulose and lignin gasification. Fuel 2014;118:250–6. https://doi.org/10.1016/j.fuel.2013.10.080.